**Advances in Computational Design**, *Vol. 10, No. 2 (2025) 111-125*
https://doi.org/10.12989/acd.2025.10.2.111


# Numerical evaluation of deoxygenation towers under blast loadings

Haijun Deng[1], Li Qin[1], Yingna Zhang[1], Tian Zuo[1] and Huilei Zhao*[2]

[1]*China Petroleum Engineering & Construction Corporation, Beijing Branch*
[2]*Beijing Datong Rising Engineering Software Development Co., Ltd*

*(Received December 23, 2024, Revised February 4, 2025, Accepted February 12, 2025)*

**Abstract.** Onshore facilities in the oil and gas industry are high risk structures because of their exposure to hazardous and flammable hydrocarbon materials, which can lead to fire and explosion accidents. Deoxygenation towers, typically made from steel plates with strengthening rings, are one of the common onshore facilities. In the literature, evaluations of onshore facilities subjected to fire or explosion actions were mainly on storage tanks with large diameters but shorte heights, while little research was conducted for deoxygenation towers. Therefore, this paper investigates the response of the deoxygenation tower subjected to blast loadings. Prototype towers with four different heights commonly used in onshore facilities in China were selected. Nonlinear finite element models were developed for the prototype towers with rate-dependent plasticity materials. Implicit dynamic analyses were performed with the input of blast loading. The blast loading was applied as a pressure wave on the tower surface which changes with location and time. The tower structural responses were evaluated in terms of roof drift, base shear, and plastic strain. By comparing the maximum demands with the code limits, it can be concluded that in general, the tower structures can withstand the pressure from explosion accidents with considerable damage, particularly local buckling of the steel plate.

**Keywords:** blast loading; deoxygenation towers; nonlinear dynamic analyses; wave pressure

## 1. Introduction

Onshore facilities in the oil and gas industry are high risk structures because of their exposure to hazardous and flammable hydrocarbon materials. In the petrochemical industry, there are many storage tanks storing flammable and explosive hazardous chemicals. Once the leakage of hazardous chemical substances occurs, it is prone to cause fire and explosion accidents. When the primary accident propagates to nearby facilities, the accident consequences could expand and trigger a so-called domino effect. Although such incidents may be relatively rare, when they do occur the consequences can be extremely severe involving personnel casualty and financial loss and potentially impacting public safety. Therefore, it is important to design the onshore facilities against the blast loading. Historically, blast resistant design technology in the petrochemical industry has evolved from equivalent static loads and conventional static design methods

*Corresponding author, Professor, E-mail: zhaohl@datongrising.com


 ISSN: 2383-8477 (Print), 2466-0523 (Online)

(Bradford and Culbertson 1967, You *et al*. 2023, Sari and Korkmaz 2024), to simplified dynamic design methods that take into account dynamic characteristics and ductility of structural components, and based on TNT equivalent blast loading (Forber 1998), and finally to more complex and rational methods involving vapor cloud explosion models to characterize the blast loading and nonlinear multi-degree of freedom dynamic models to analyze the infrastructures. The ASCE 41088 (2010) (Design of Blast-Resistant Buildings in Petrochemical Facilities) provides guidelines on the various methods available for the structural design of blast resistant buildings in petroleum and chemical process plants. Although the ASCE 41088 (2010) mainly focuses on the building structures, it can provide guidance on the blast loadings and analyses for non-building facilities, such as denitrification, deoxygenation, and desulfurization towers, typically made from steel shells with strengthening rings.

Several types of explosions are considered in ASCE 41088 (2010) including Vapor Cloud Explosions, Pressure Vessel Explosions, Condensed Phase Explosions, and Dust Explosions according to the causes of explosion accidents. Two types of blast waves can be generated from the explosion: the shock and pressure wave. The shock wave is characterized by an instantaneous increase in pressure and is referred to as detonation with a propagation velocity of the shock wave above the speed of sound. This detonation could be generated from pressure vessel, dust explosion, or explosion of TNT equivalent materials (Rosin *et al*. 2024). On the other hand, most vapor cloud explosions are characterized by slow deflagration and propagate in the form of pressure waves that usually travel below the speed of sound, which is slower in comparison to shock waves. Most vapor cloud deflagrations typically generate pressure waves on the near field facilities (AICE 2010) (Sharma 2020).

Several parameters are needed to define the blast wave pressure including the peak positive overpressure, peak negative pressure, reflection coefficient, dynamic pressure, shock front velocity, and blast wavelength. The blast wave attenuates as it propagates outward from the explosion epicenter. Consequently, the values of peak overpressure and impulse decrease with distance while the duration tends to increase. Values for these blast wave parameters can be determined from published data in the form of scaled values (overpressure, impulse or duration) as a function of scaled distance (UFC 3-340-02 2008) (Van den Berg 1985) (CCPS 1994). When the free field blast wave from an explosion strikes a surface, it is reflected. The effect of this blast wave reflection is that the surface will experience a pressure much more than the incident side-on value. The pressure amplification can be determined from the reflection coefficient which can be determined from a simple formula. The shock velocity and blast wavelength can be used to determine the duration of the blast. The determination of these parameters can be from the analytical and empirical equations (Rosin *et al*. 2024) (Godoy and Ameijeiras 2023) (Duong *et al*. 2012). The blast waves can also be characterized from computational fluid dynamics (CFD) analyses, which are commonly adopted in blast resistance research for storage tanks (Li *et al*. 2022, Zhang *et al*. 2015, Saifi *et al*. 2024, Wang *et al*. 2023).

Design of structures to resist the effects of accidental explosions at petrochemical plants requires knowledge of the dynamic properties of structural materials as well as the allowable responses of components and systems. Also, sustainability of construction materials is considered (Sandybay *et al*. 2024, Ualiyev *et al*. 2024a, Kozhageldi *et al*. 2023, Omarova *et al*. 2024). Materials and structural systems respond differently to dynamic loads produced by explosions than to statically applied conventional loads and it is imperative that the engineer understand these differences. These differences are inertial, damping, and strain-rate effects, which cause dynamic response amplifications. In the research work on the blast loading resistance, the structural

material is mainly modeled with advanced material constitutive models such as rate-dependent Perzyna model (Perzyna 1980), Cowper–Symonds model (Lu *et al*. 2019, Lai *et al*. 2021, AL-Yacouby *et al*. 2021), Modified Cowper–Symonds model (Li *et al*. 2022), Johnson-Cook model (Zhang *et al*. 2018), and Concrete Damage model (Lee *et al*. 2016, Zaid and Sadique 2020). These material models can consider dynamic, temperature effects on the material strength as well as plastic behavior.

Several dynamic analysis methods are available for determining the dynamic response of the structures subjected to blast loading ranging from simple hand calculations and graphical solutions to more complex computer-based applications. The ASCE 41088 (2010) recommends several methods. The first one is equivalent static method. As the name implies, this method employs a static analysis with an approximate applied load to simulate the dynamic response. This is sometimes called an "equivalent wind" approach. The primary difficulty with this method is determining an appropriate static loading which will yield reasonable results. This method is not recommended for general use except for cases where the structure is far removed from the blast source, such that the blast loading resembles a wind gust. The second method is to conduct dynamic analyses on a single degree of freedom (SDOF) model. This method greatly simplifies the dynamic analysis effort compared to that of structures having distributed mass. The procedure for obtaining an equivalent SDOF approximation for a structural component is based on its deformed shape under the applied loading and the strain energy equivalence between the actual structure and the SDOF approximation. Equivalent mass, stiffness and loading are obtained through the use of transformation factors. These factors can be determined by assuming deflection shape functions through a so-called generalized degree of freedom model. The solutions for the SDOF system can be derived from graphic solution, closed form solution, and numerical integration. Another method is to use multi-degree of freedom model systems. Nonlinear dynamic finite element analyses can be conducted for the multi-degree of freedom model to obtain the dynamic response of the structure. Through these analyses, the following responses need to be evaluated to a given blast load: maximum deflection, plastic deformation, dynamic reactions, and rebounding deflections. In the research work on the structural blast analyses, sophistical three-dimensional (3D) models were often constructed in commercial finite element software, such as LS-DYN (Rosin *et al*. 2024, Lu *et al*. 2019, Lai *et al*. 2021, ANSYS (AL-Yacouby *et al*. 2021, Lee *et al*. 2016, Ajan *et al*. 2023) or Abaqus (Sharma 2020, Godoy and Ameijeiras 2023, Zhang *et al*. 2018). Explicit and implicit dynamic analyses were typically used for structures subjected to blast waves. The blast waves were generated from computational fluid dynamic analyses or analytical and empirical equations (Saifi *et al*. 2024).

The research work for the onshore facilities subjected to blast loadings was conducted mainly on storage tanks (Rosin *et al*. 2024). The studies on the storage tanks were conducted mainly through explicit and implicit dynamic analyses with wave shocks generated from the CFD analysis or empirical equation. From these studies, the behavior of the tank under blast loading was evaluated in terms of deformation, plastic strain, equivalent stress, and energy absorptions. In general, the liquid inside the tank can effectively enhance the structural resilience against potentially catastrophic blasts as it can help absorb energy generated from the blast. Besides the traditional blast loading, Li *et al*. (2022) considers the coupling effect of the blast loading and the fire while Lai *et al*. (2021) incorporates the fragment impact with the blast loading. From Li *et al*. (2022), the fire can cause high temperatures and absorb more impact energy during the blast, but it can also reduce the material strength. From Lai *et al*. (2021), overall damage of the storage tank subjected to the coupling effect is more severe than that caused by blast waves and fragment

Table 1 Geometry of the tower

| [mm] | Base Segment | Interior Segment | Cap roof | Strengthening ring |
|---|---|---|---|---|
| Diameter | 3000 | 3000 | 3000 | 3000 |
| Thickness | 32* | 16 | 16 | 16 |
| Height | 3700 | 2000 | 750 | 75 |

* Value at the base and tamped as going up

Table 2 Material properties

| Elastic Modulus | Poisson's ratio | Yield Str. | Fracture Str. | Ult. strain | Tan. Modulus |
|---|---|---|---|---|---|
| E (GPa) | u | $f_y$ (MPa) | $f_u$ (MPa) | $e_u$ | $E_t$ (MPa) |
| 200 | 0.3 | 260 | 485 | 0.15 | 1513 |

separately. Little research was performed for denitrification or deoxygenation towers. However, similar research methods on the blast loading and structural material modeling can be used for the towers as they share similar structural shape (thin-walled cylindrical geometry) and material properties (structural steels) as the storage tanks. Therefore, this paper presents a study on the response of deoxygenation towers under the blast loadings using nonlinear dynamic analyses.

## 2. Towers structures and models

### *2.1 Tower geometry and material*

The commonly used deoxygenation tower in the oil and gas industry in China typically has several structural components: base segment, interior segment, roof caps, and strengthening rings as shown in Fig.1a. The roof cap and interior segments are made from steel plates with a thin thickness (t) while the base segment typically has an increased thickness ($t_b$) to resist overturning moment from the wind. Strengthening rings are typically in place between each segment for overall stability of the tower. The number (N) of segments including the base ranges from 4 to 10 in typical constructions. This paper investigates the deoxygenation tower with four different numbers of segments (N=4, 6, 8, and 10). The geometries of the studied tower are shown in Table 1. The structural components are all made from structural steel SA 516-70. The material properties are shown in Table 2. The tower structure is typically anchored to a solid concrete foundation made from sustainable materials (Onopriyenko *et al*. 2025, Manap *et al*. 2025, Ualiyev *et al*. 2024b, Kissambinova *et al*. 2022, Syzdykov *et al*. 2022, Kozhageldi *et al*. 2022, Aitbayeva *et al*. 2022), which can be approximately considered as fixed conditions.

### *2.2 Nonlinear tower models*

Three-dimensional (3D) nonlinear finite element models were developed for the tower in the general-purpose finite element software ANSYS. As shown in Fig. 1b, the base, interior, and roof segments are modeled with 3D shell elements while the strengthening rings are modeled with 3D beam elements with an approximately uniform mesh size of 100 mm. The fixed boundary

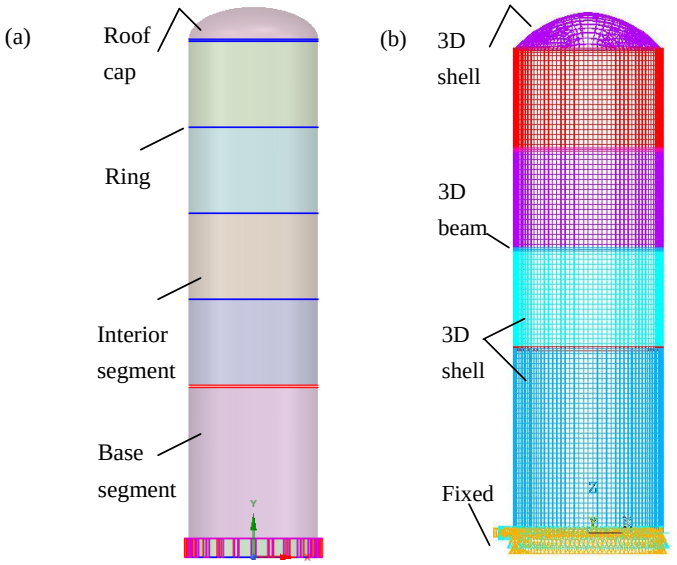


Fig. 1 Deoxygenation tower: (a) Structural components; (b) 3D model

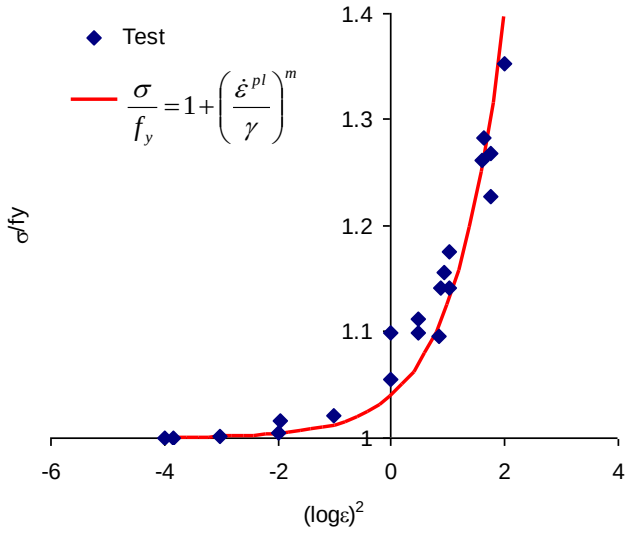


Fig. 2 Perzyna model parameter calibration

conditions are applied at the base of the tower. The rate-dependent plasticity material model is used since the blast loading typically is considered as extreme loading and occurs in a very short duration (10 to 100 ms). The material model used in this study combines viscoplasticity with bilinear isotropic strain hardening rules (Ajan *et al*. 2023, Onopriyenko *et al*. 2025, Utemuratova *et al*. 2024, Sharipkhan *et al*. 2024a, b). The bilinear isotropic strain hardening parameters are set as the yield strength and tangent modulus shown in Table 2. The viscoplasticity is modeled with the Perzyna model (Perzyna 1980). The material strain rate hardening (m) and material viscosity ($\mu$) parameters were calibrated from test results on the structural steel as shown in Fig. 2. The final calibrated parameters are as follows: m=0.25 and $\gamma$ = 400000.

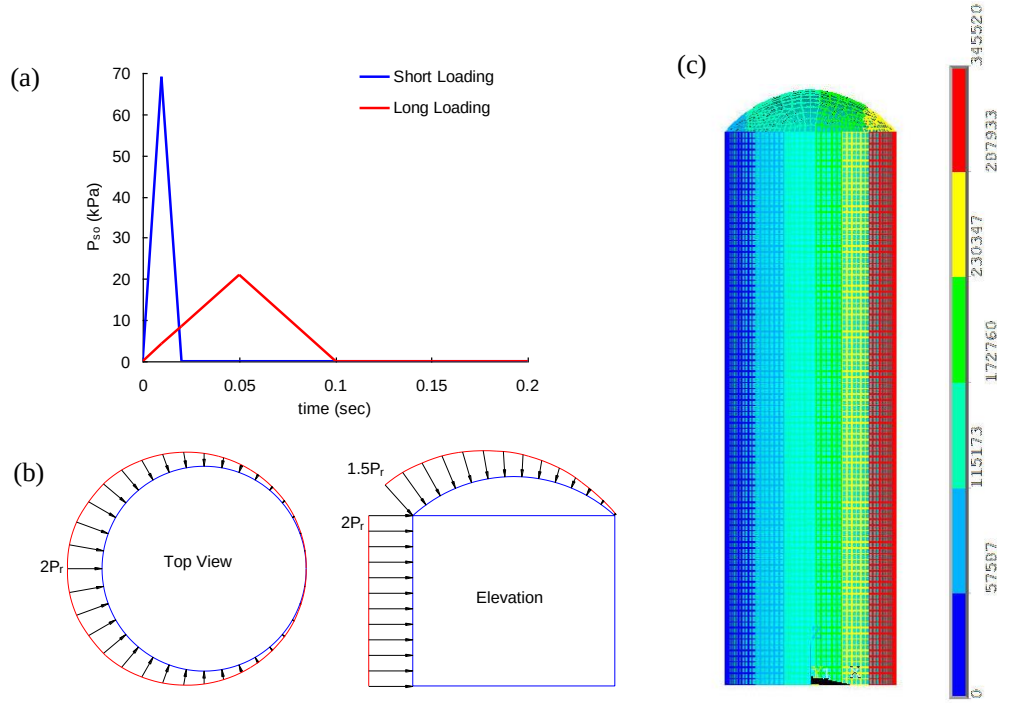


Fig. 3 Blast loading modeling: (a) Pressure waves; (b) pressure distribution; (c) application of the pressure on the model

### *2.3 Modeling of blast loadings*

For the onshore facilities, the Vapor Cloud Explosion is the most common type of explosion. Considering typical distances among equipment and structures, pressure waves will most likely be imposed on the tower body and roof during the explosion accident (Van den Berg 1985). For the design and analysis of onshore facilities against the blast loading, the ASCE 41088 (2010) recommends considering two loading scenarios: (1) high pressure ($P_{so}$=69 kPa) with short duration ($t_0$=20 ms), termed here as short loading and (2) low pressure ($P_{so}$=21 kPa) with long duration ($t_0$=100 ms), termed here as long loading (See Fig. 3a). The reflection factor ($C_r$) is also taken into account to amplify the maximum pressure ($P_r$=$C_rP_{so}$), where $C_r$ can be estimated as 2+0.0073$P_{so}$. The generated wave pressure is not constant on the tower surface since the side directly facing the explosion source should have a high pressure while the pressure will reduce as moving towards other side of the tower. Following the ASCE 41088, the pressure varying patterns on the tower surfaces are shown in Fig. 3b, where the pressure is assumed as constant along the height of the tower but varying nonlinearly on the circumference direction of the tower body and roof cap. The variations follow Eqs. (1) and (2) for the tower body and roof cap, respectively. The applied pressure contour on the 3D model is shown in Fig. 3c.

$$P = P_r(1 + cos\theta) \tag{1}$$

$$P = P_r(1 + \sqrt{2}sin\theta) \tag{2}$$

Table 3 Fundamental period and damping coefficient

| N = | 4 | 6 | 8 | 10 |
|---|---|---|---|---|
| Fundamental period (s) | 0.040 | 0.068 | 0.110 | 0.163 |
| Mass coefficient (a) | 6.993 | 4.156 | 2.758 | 1.913 |
| Stiffness coefficient (b) | 0.0001 | 0.00016 | 0.0002 | 0.0002 |

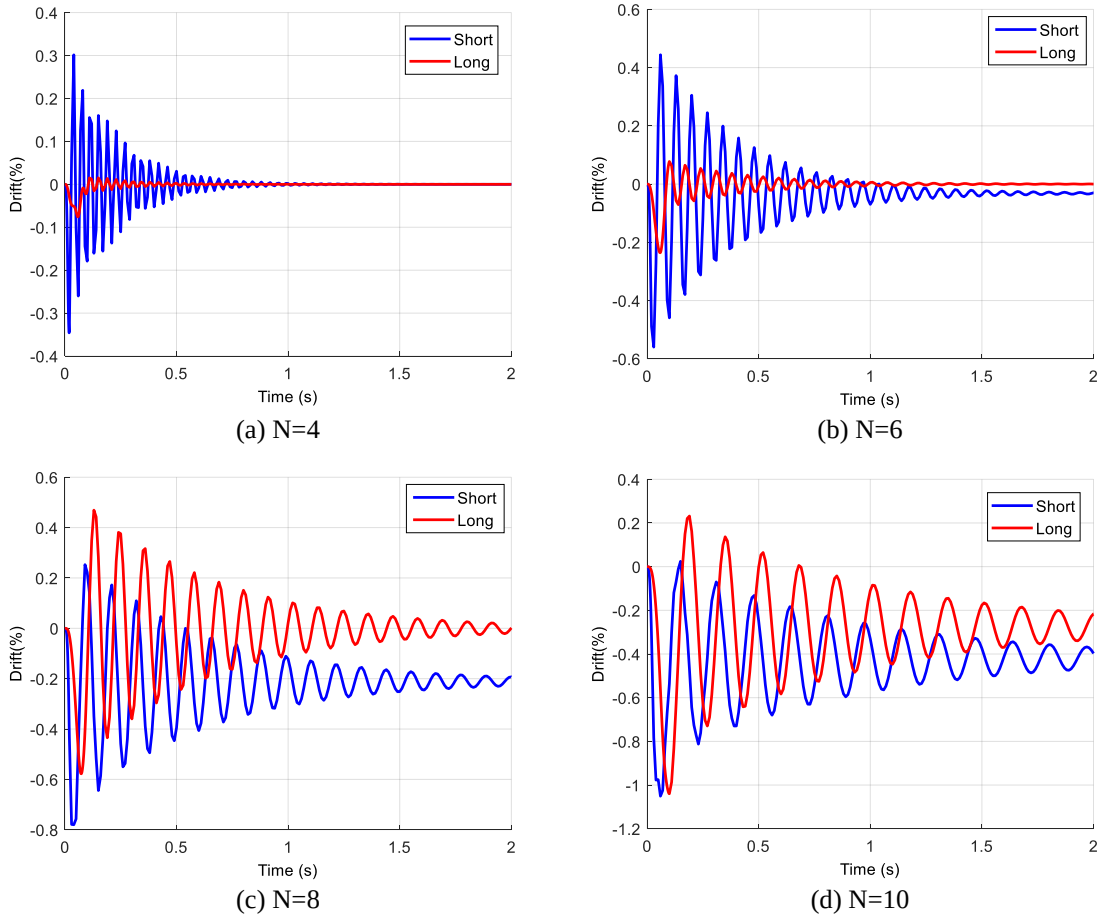


(a) N=4 (b) N=6

(c) N=8 (d) N=10

Fig. 4 Roof drift time history

### *2.4 Dynamic analysis procedure*

The dynamic analyses were conducted using time steps of 0.0002 second for the short loading and 0.001 second for the long loading during the forced vibration stage. The time step increases to 0.01 second during free vibration stage till a total simulation time of 2 second. The time-stepping technique is the Newmark integration method (using integration coefficients of 0.25 and 0.5) with two sub-steps per time step (Aidyngaliyev *et al*. 2024). The nonlinear solving technique is a modified Newton-Raphson iteration method with a force tolerance error of 0.5% (Zhang *et al*.

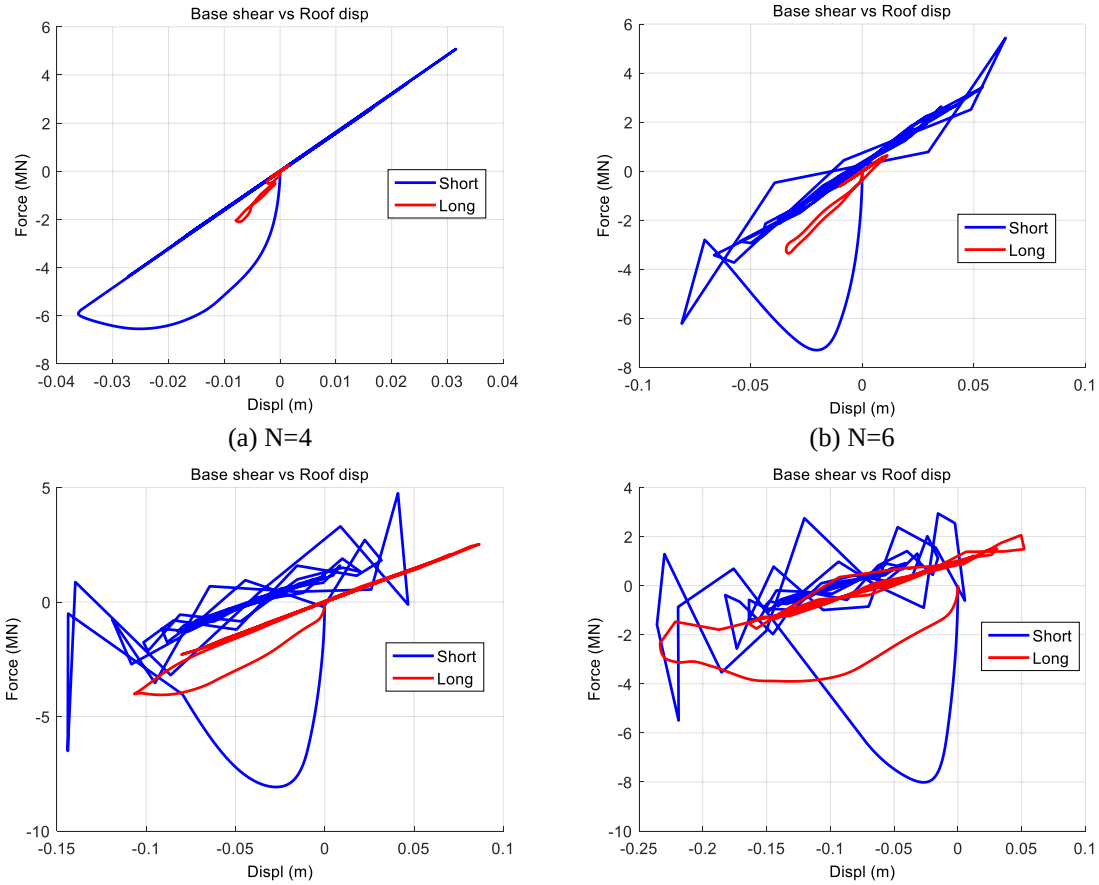


(a) N=4 (b) N=6

(c) N=8 (d) N=10

Fig. 5 Base shear vs. roof displacement

2024). Both material and geometry nonlinearities were considered in the simulations. Rayleigh damping is used with an equivalent damping ratio (z=3%) anchored at the first (fundamental) and last significant horizontal vibration modes when the cumulative mass participation ratio exceeds 99%. The Rayleigh damping coefficients were determined through modal analyses performed on the 3D models with initial stiffness using Eqs. (3) and (4). The fundamental vibration periods and calculated Rayleigh damping coefficients are listed in Table 3.

$$a = 2z w_i w_j/(w_{i+}w_j) \tag{3}$$

$$b = 2z/(w_1+w_7) \tag{4}$$

## 3. Numerical results

Fig. 4 shows the roof drift time history for different heights of the tower (N = 4 to 10) under two types of blast loading conditions. The roof drift was calculated by normalizing the roof

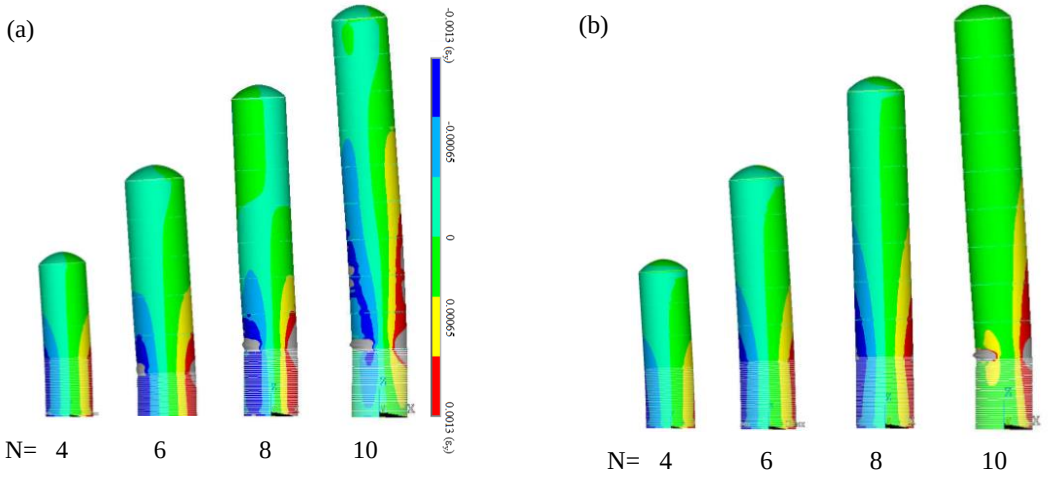


(a) N=4 (b) N=6

Fig. 6 Normal strain along the height of tower: (a) short loading; (b) long loading

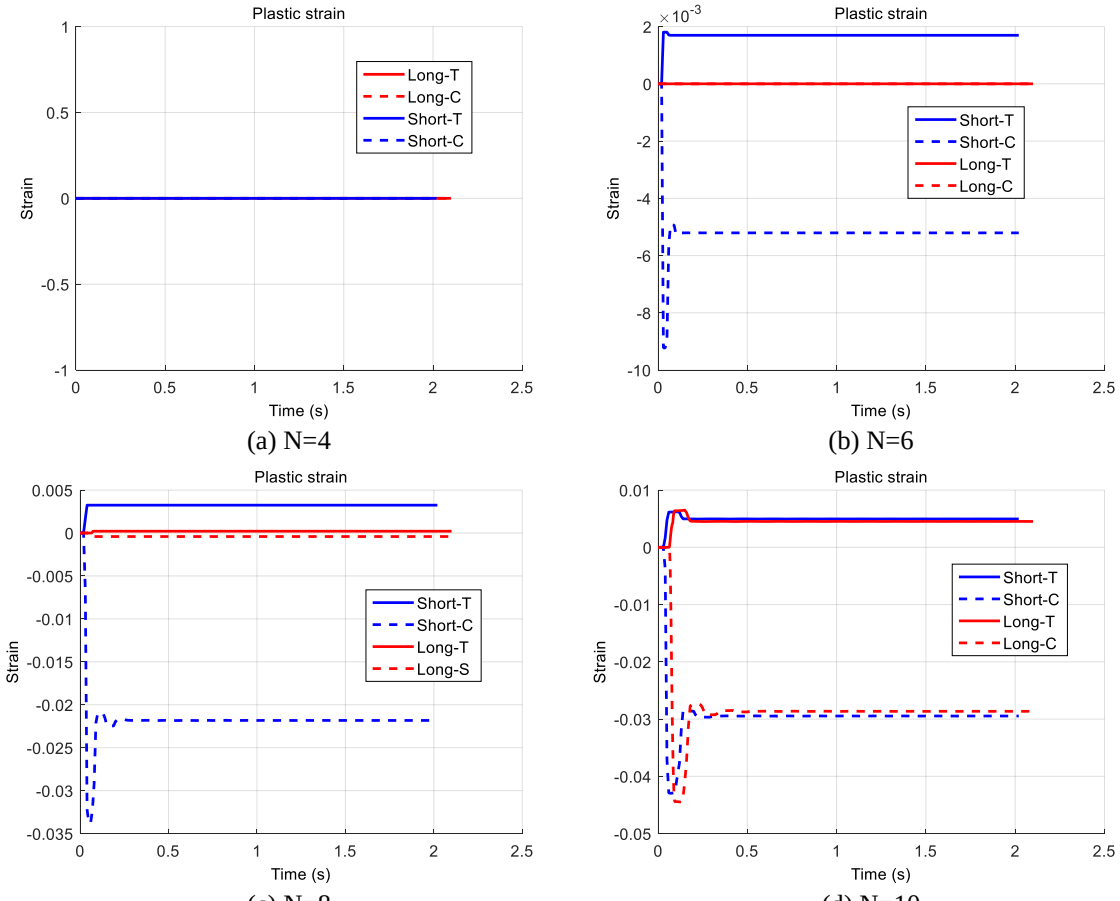


(a) N=4 (b) N=6

(c) N=8 (d) N=10

Fig. 7 Maximum plastic strain history

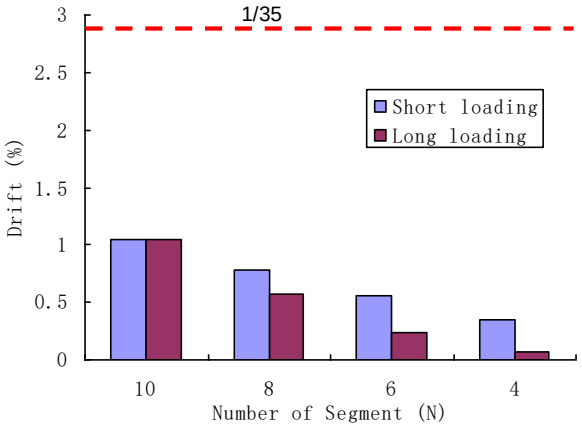


Fig. 8 Maximum roof drift demand

displacement with the height of the tower (D/H). In general, the roof drift increases as the height of the tower increases due to the increase of the overturning effect. For short towers, the short loading case creates a much higher roof drift demand than the long loading case does. However, for tall towers, particularly when N = 10, the long loading case generates similar roof drift demand as the short loading case though it has a much smaller peak pressure wave (refer to Fig. 3a). For a given amount of time, more vibration cycles are observed for short towers possibly due to their relatively shorter vibration period as compared to the tall towers. This fact indicates that more time is needed for tall towers to settle down.

Fig. 5 shows the hysteresis response (base shear force vs. roof displacement) for different heights of the tower (N=4 to 10) under two types of blast loading conditions. In general, the short loading cases incur much larger base shear force demand than the long loading cases. This trend is possibly due to the higher applied pressure and faster loading rate in the short loading cases. The taller towers (N=8 and 10) exhibit more inelastic response than the short towers.

Fig. 6 shows distributions of the normal strain along the height of the tower under: (a) short loading; (b) long loading at the time when the roof drift reaches maximum. The contour is limited at the yield strain of the steel so that the grey area indicates the yielding region. The largest strain demand (tension on one side and compression on the other) occurs nearby the interface between the base and 1$^{st}$ interior segment due to the increase of the base steel plate. In general, the short loading cases result in more yielding on the tower than the long loading cases. The short tower (N=4) remains elastic under both loading conditions.

Fig. 7 shows the maximum plastic strain (T-tension and C-compression) time history for different heights of the tower (N = 4 to 10) under two types of blast loading conditions. As the tower becomes taller (N increases), large plastic strain demands are observed. Also, the short loading cases induce larger plastic response on the tower than the long loading cases. The compressive plastic strain demand is significantly higher than the tensile plastic strain demand, possibly due to the local buckling of the steel plate.

## 4. Demand evaluation

The ASCE 41088 (2010) recommends a roof drift limit of 1/35 for the onshore facilities under

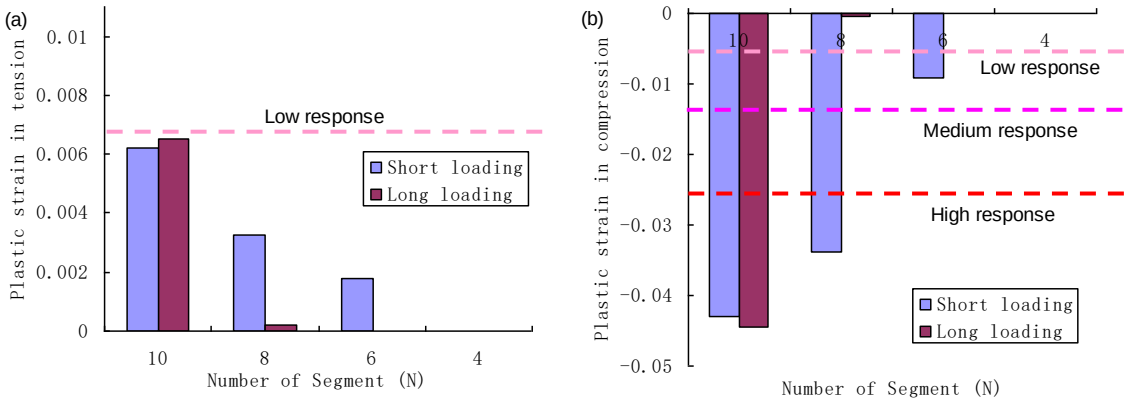


Fig. 9 Maximum plastic strain: (a) tensile; (b) compressive

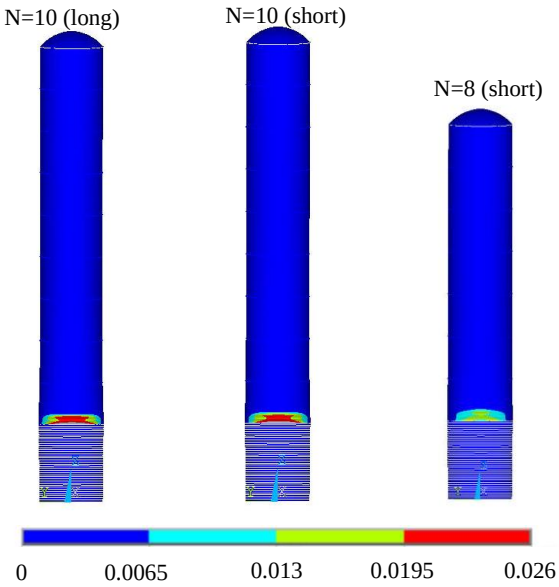


Fig. 10 Blast loading modeling: (a) Pressure waves; (b) pressure distribution; (c) application of the pressure on the model

blast loading to ensure overall structural stability. At the same time, the code also provides plastic response limits for three response levels (low, medium, and high). The corresponding limits for the plastic strain in the steel plate are 0.0065, 0.013, 0.026 for low, medium, and high response levels, respectively (ASCE 41088 2010).

Fig. 8 shows the maximum roof drift demand for the cases studied. As a reference, the code limit (1/35) was plotted as a horizontal trendline. It can be seen from Fig. 8 that the maximum roof drift demand is much less than the code limit which indicates the overall stability of the tower under the blast loadings.

Fig. 9 shows the maximum plastic strain demand for the cases studied: (a) tensile; (b) compressive. As a reference, the code limits for low, medium, and high response levels were

plotted as horizontal trendlines. As seen in Fig.9a, the tensile plastic strain demand is below the low response limit. However, for the compressive plastic strain shown in Fig. 9b, the demand in taller towers (N=8 and 10) is higher than the high response limit. This high plastic strain demand can be originated from the local buckling of the steel plate. Figure 10 shows the equivalent plastic strain contour for the three cases with high compressive plastic strain demand: N=10 under long loading; N=10 under short loading; and N=8 under short loading. As seen, only a small region near the top of the base segment shows higher plastic strain demand than the code low response limit, which indicating local buckling in this region.

## 5. Conclusions

This paper presents a numerical study for deoxygenation towers subjected to blast loadings. Four typical tower configurations commonly seen in the oil-gas industry in China were selected for the evaluation. The evaluation was conducted via time history analyses on nonlinear structural tower models under two types of blast loading pressures. The following conclusions can be made from the numerical results:

1. The taller towers typically incur large demand due to the larger overturning effect.
2. The short loading cases in general create a higher structural response than the long loading cases except for the N=10 tower where the structural response is similar for both cases.
3. The towers exhibit higher strength under the short loading cases due to the strain rate effect.
4. Nonlinear structural responses are observed near the interface between the base and 1$^{st}$ exterior segments possibly due to the increase of the plate thickness at the base segment.
5. The tower exhibits a much higher plastic strain in compression regions than that in tension regions which indicates possible local buckling of the steel plate.

The maximum structural demands obtained from the numerical analyses were compared with the code limits specified in ASCE 41088 with the following findings:

1. The maximum drift of the tower is less than the code limit which indicates the overall stability of the structure under blast loadings.
2. The maximum tensile plastic strain is within the low response limit indicating an unlikely tensile fracture of the steel plate during the explosion.
3. The maximum compressive plastic strain exceeds the high response limit for three cases. These exceedances occur at very limited regions indicating local buckling in the steel plate.

## Acknowledgements

Funding source: Safety analysis of oil field equipment under the action of explosion shearing load based on finite element method, CPECCBJIT / 2024/S10.

## References

American Institute of Chemical Engineers (2010), *Guidelines for Vapor Cloud Explosion, Pressure Vessel Burst, BLEVE, and Flash Fire Hazards, (2nd Edition)*, Wiley: Hoboken, NJ, U.S.A.

ASCE 41088 (2010), Design of blast-resistant buildings in petrochemical facilities, Task Committee on

Blast-Resistant Design of the Petrochemical Committee of the Energy Division of ASCE, Reston, Virginia, U.S.A.

Al-Yacouby, A.M., Hao, L.J., Liew, M.S., Ratnayake, R.C. and Samarakoon, S.M. (2021), "Thin-walled cylindrical shell storage tank under blast impacts: Finite element analysis", *Materials*, **14**(22), 7100. https://doi.org/10.3390/ma14227100.

Aitbayeva, A., Shon, C.S., Zhang, D. and Kim, J.R. (2021), "Assessment of recycled toilet bowl wastes as pozzolanic materials: Material characterization and performance of mortar mixtures", *Mater. Sci. Forum*, **1023**, 135-140. https://doi.org/10.4028/www.scientific.net/MSF.1023.135

Aidyngaliyev, I., Zhang, D., Fleischman, R., Shon, C.S. and Kim, J. (2024), "Structural response of a three-story precast concrete structure subjected to local diaphragm failures in a shake table test", *Comput. Concr.*, **33**(2), 195-204. https://doi.org/10.12989/cac.2024.33.2.195

Ajan, B., Zhang, D., Spitas, C., Abou Fakhr, E. and Wei, D. (2023), "Geometry optimization of a double-layered inertial reactive armor configured with rotating discs", *Adv. Comput. Des.*, **8**(4), 309-325. https://doi.org/10.12989/acd.2023.8.4.309.

Bradford and Culbertson (1967), "Design of control houses to withstand explosive forces", *Loss Prevent.*, **1**, 28-30.

CCPS Explosion Guidelines (1994), Guidelines for evaluating the characteristics of vapor cloud explosions, flash fires, and BLEVEs, center for chemical process safety, American Institute of Chemical Engineers, New York, NY, U.S.A.

Duong, D.H., Hanus, J.L., Bouazaoui, L., Regal, X., Prod'Homme, G., Noret, E., Yalamas, T., Reimeringer, M., Bailly, P. and Pennetier, O. (2012), "Response of a tank under blast loading–Part II: experimental structural response and simplified analytical approach", *Eur. J. Environ. Civil Eng.*, **16**(9), 1042-1057. https://doi.org/10.1080/19648189.2012.699743.

Forbes D.J. (1998), "Protecting petroleum process plant buildings from vapor cloud explosions", *ACI Symposium Paper*, **175**, 53-86. https://doi.org/10.14359/5916.

Godoy, L.A. and Ameijeiras, M.P. (2023), "Plastic buckling of oil storage tanks under blast loads", *Structures*, **53**, 361-372. https://doi.org/10.1016/j.istruc.2023.04.057.

Kissambinova, A., Shon, C.S., Bazarbekova, A., Sandybay, S., Zhang, D. and Kim, J.R. (2022). "High sulfate-bearing kaolin clay stabilization with waste glass powder before and after mellowing process", *Key Eng. Mater.*, **920**, 232-238. https://doi.org/10.4028/p-2y75dh

Kozhageldi, N., Shon, C.S., Kareken, G., Tukaziban, A., Mardenov, M., Zhang, D. and Kim, J.R. (2023). "Properties of geopolymer mortar mixtures containing waste glass aggregates and river sand", *Key Eng. Mater.*, **945**, 93-99. https://doi.org/10.4028/p-67b121.

Kozhageldi, N., Shon, C.S., Yerbolat, I., Orynbassarov, I., Zhang, D. and Kim, J.R. (2022), "Thermal performance evaluation of non-autoclaved aerated concrete produced with crushed waste glass bottle aggregate and glass fiber", *Mater. Sci. Forum*, **1077**, 243-249. https://doi.org/10.4028/p-1689hp

Li, X., Chen, G., Khan, F., Lai, E. and Amyotte, P. (2022). "Analysis of structural response of storage tanks subject to synergistic blast and fire loads", *J. Loss Prevent. Proc. Ind.*, **80**, 104891. https://doi.org/10.1016/j.jlp.2022.104891.

Lee, S.W., Choi, S.J. and Kim, J.H.J. (2016), "Analytical study of failure damage to 270,000-kL LNG storage tank under blast loading", *Comput. Concr.*, **17**(2), 201-214. https://doi.org/10.12989/cac.2016.17.2.201.

Lu, S., Wang, W., Chen, W., Ma, J., Shi, Y. and Xu, C. (2019), "Behaviors of thin-walled cylindrical shell storage tank under blast impacts", *Shock Vib.*, **1**, 6515462. https://doi.org/10.1155/2019/6515462.

Lai, E., Zhao, J., Li, X., Hu, K. and Chen, G. (2021), "Dynamic responses and damage of storage tanks under the coupling effect of blast wave and fragment impact", *J. Loss Prevent. Proc. Ind.*, **73**, 104617. https://doi.org/10.1016/j.jlp.2021.104617.

Manap, I., Galymzhankyzy, A., Omarova, Z., Ualiyev, D., Temirbekov, D., Shon, C.S., Zhang D. and Kim, J.R. (2025), "Can geopolymer mixture be a solution for utilizing waste glass and basic oxygen furnace slag as aggregates?", *In E3S Web Conferences*, **612**, 04001. https://doi.org/10.1051/e3sconf/202561204001.

Ogwumeh, C.M., Zhang, D., Shon, C.S., Lee, D. and Kim, J. (2025), "Experimental study on seismic performance of unreinforced masonry walls retrofitted with low-strength engineered cementitious composites", *Bulle. Earthq. Eng.*, **1**(22). https://doi.org/10.1007/s10518-025-02138-5.

Omarova, Z., Ualiyev, D., Shon, C.S., Zhang, D. and Kim, J.R. (2024), "Utilizing mineral sequestration technology for enhanced performance of concrete containing basic oxygen furnace slag", *In E3S Web Conferences*, **579**, 02002. https://doi.org/10.1051/e3sconf/202457902002.

Onopriyenko, Z., Shon, C.S., Zhang, D. and Kim, J.R. (2025), "Compressive strength and expansion characteristics of BOFS-Based geopolymer mortar under different curing regimes", *Proceedings of the International Conference on Manufacturing, Material and Metallurgical Engineering*, 217-226. https://doi.org/10.1007/978-3-031-78295-4.

Perzyna, P. (1980), "Modified theory of viscoplasticity. Application to advanced flow and instability phenomena", *Arch. Mech.*, **32**, 403-420.

Rosin, J., Stocchi, A., Bruckhaus, N., Heyner, J., Weidner, P. and Waas, T. (2024), "Cylindrical steel tanks subjected to long-duration and high-pressure triangular blast load: current practice and a numerical case study", *Appl. Sci.*, **14**(8), 3465. https://doi.org/10.3390/app14083465.

Sharma, R.K. (2020), "A violent, episodic vapour cloud explosion assessment: Deflagration-to detonation transition", *J. Loss Prev. Process Ind.*, **65**, 104086. https://doi.org/10.1016/j.jlp.2020.104086.

Saifi, F., Anas, S.M., Tahzeeb, R., Shariq, M. and Alam, M. (2024), "Numerical investigation of blast loading effects on a thin-walled cylindrical steel storage tank", *Mater. Today Proceedings*, 4 April 2024. https://doi.org/10.1016/j.matpr.2024.04.001.

Sharipkhan, N., Clifford, O., Perveen, A., Zhang, D. and Wei, D.M. (2024a), "Investigation of co-extrusion using a coat hanger die with different feedblock cross-section", *Key Eng. Mater.*, **973**, 131-137. https://doi.org/10.4028/p-RcTKV4

Sari, A. and Korkmaz, K. (2024), "An analytical approach for offshore structures considering soil-structure interaction", *Adv. Comput. Des.*, **9**(1), 25-38. https://doi.org/10.12989/acd.2024.9.1.025.

Sandybay, S., Orynbassarov, I., Shon, C.S., Zhang, D. and Kim, J.R. (2024), "Performance assessment of basic oxygen furnace slag (BOFS) as an ice-melting abrasive material", *Mater. Sci. Forum*, **1127**, 57-64. https://doi.org/10.4028/p-LNmK9v.

Sharipkhan, N., Perveen, A., Zhang, D. and Wei, D.M. (2024b), "Investigation of the two-channel feedblock zone in co-extrusion of polymers", *Key Eng. Mater.*, **973**, 119-129. https://doi.org/10.4028/p-RN5jhP

Syzdykov, D., Shon, C.S., Sandybay, S., Orynbassarov, I., Zhang, D. and Kim, J.R. (2022), "Preliminary investigation of geopolymer mixture using GGBFS and off-ASTM class F fly ash", *Mater. Sci. Forum*, **1053**, 309-314. https://doi.org/10.4028/p-mx9n06

Van den Berg, A.C. (1985), "The multi-energy method - a framework for vapor cloud blast prediction", *J. Hazard. Mater.*, **12** (1), 1-10. https://doi.org/10.1016/0304-3894(85)80022-4.

UFC 3-340-02 (2008), Structures to resist the effects of accidental explosions, unified facilities criteria 3-340-02 (formerly Technical Manual TM 5-1300), U.S. Department of Defense, Washington, DC, USA.

Ualiyev, D., Galymzhankyzy, A., Manap, I., Omarova, Z., Temirbekov, D., Tukaziban, A. and Zhang, D. (2024a), "Effect of recycled waste PET bottle fibers on mechanical properties of geopolymer mixtures containing crushed waste glass sands", *Key Eng. Mater.*, **979**, 117-123. https://doi.org/10.4028/p-7qdQwk.

Ualiyev, D., Omarova, Z., Shon, C.S., Zhang, D. and Kim, J.R. (2024b), "Effects of curing conditions, age, and particle size on $CO_2$ sequestration of basic oxygen furnace slag used in concrete", *Key Eng. Mater.*, **986**, 17-24. https://doi.org/10.4028/p-BPO57b.

Utemuratova R., Karabay A., Zhang D., Varol H.A. (2024), "Shear design optimization of short rectangular reinforced concrete columns using deep learning", *Lecture Notes Civil Eng.*, **369**, 205-216. https://doi.org/10.1007/978-981-99-4049-3_18.

You, Y.S., Sun, M.Y. and Lee, Y.H. (2023), "Design and analysis of offshore wind structure", *Adv. Comput. Des.*, **8**(3), 191-217. https://doi.org/10.12989/acd.2023.8.3.191.

Wang, Y., Wu, W., Kim, J. and Zhang, D. (2023), "Class-A prediction of debris flow impact against rigid obstacles", *Proceedings of the 84th EAGE Annual Conference & Exhibition*, **2023**(1), 1-5, European Association of Geoscientists & Engineers, Vienna, June.

Zaid, M. and Sadique, M.R. (2020), "Numerical modelling of internal blast loading on a rock tunnel", *Adv. Comput. Des.*, **5**(4), 417-443. https://doi.org/10.12989/acd.2020.5.4.417.

Zhang, B.Y., Li, H.H. and Wang, W. (2015), "Numerical study of dynamic response and failure analysis of spherical storage tanks under external blast loading", *J. Loss Prevent. Proc. Ind.*, **34**, 209-217. https://doi.org/10.1016/j.jlp.2015.02.008.

Zhang, R., Jia, J., Wang, H. and Guan, Y. (2018), "Shock response analysis of a large LNG storage tank under blast loads", *KSCE J. Civil Eng.*, **22**, 3419-3429. https://doi.org/10.1007/s12205-017-1246-x.

Zhang, Z., Feng, Y., Zhang, D. and Pan, Z. (2024), "Application of a ductile connection system to steel MRF strengthened with hinged walls", *Steel Compos. Struct.*, **51**(5), 487-498. https://doi.org/10.12989/scs.2024.51.5.487.

*TK*